Progress In Electromagnetics Research, Vol. 163, 39–50, 2018

SVR-CMT Algorithm for Null Broadening and Sidelobe Control

Fulai Liu, Yifan Wu*, †, Han Duan†, and Ruiyan Du

Abstract—Minimum variance distortionless response (MVDR) beamformer is an adaptive beamforming technique that provides a method for separating the desired signal from interfering signals. Unfortunately, the MVDR beamformer may have unacceptably low nulling level and high sidelobes, which may lead to significant performance degradation in the case of unexpected interfering signals such as the rapidly moving jammer environments. Via support vector machine regression (SVR), a novel beamforming algorithm (named as SVR-CMT algorithm) is presented for controlling the sidelobes and the nullling level. In the proposed method, firstly, the covariance matrix is tapered based on Mailloux covariance matrix taper (CMT) procedure to broaden the width of nulls for interference signals. Secondly, the equality constraints are modified into inequality constraints to control the sidelobe level. By the ε-insensitive loss function for the sidelobe controller, the modified beamforming optimization problem is formulated as a standard SVR problem so that the weight vector can be obtained effectively. Compared with the previous works, the proposed SVR-CMT method provides better beamforming performance. For instance, (1) it can effectively control the sidelobe and nullling level, (2) it can improve the output signal-to-interference-and-noise ratio (SINR) performance even if the direction-of-arrival (DOA) errors exist. Simulation results demonstrate the efficiency of the presented approach.

1. INTRODUCTION

Beamforming technique is an important part of array signal processing. It is widely used in wireless communications [1], microphone array signal processing [2] and radar [3]. A typical, representative beamformer, known as minimum variance distortionless response (MVDR) or Capon beamformer [4], minimizes array output power and maintains a distortionless mainlobe response toward the desired signal. Unfortunately, the conventional MVDR beamformer may have unacceptably low and narrow null level in the direction of interference signal or high sidelobes in the case of low sample support. Moreover, it is possible that the mismatch occurs between adaptive weights and data due to the perturbation of the interference location when the antenna platform vibrates or interference moves quickly, which may lead to the nulls shift from the directions of the interference. In adaptive array systems, the aforementioned problems may contribute to performance degradation under the scenarios of unexpected interference signals.

To improve the robustness of the beamformer against unexpected interference signals, several null broadening approaches have been proposed. The null broadening method is initially proposed by Mailloux [5] and Zatman [6], which utilizes a grid of virtual and equal-power interference signals to replace the original interference. The null broadening method proposed by Mailloux and Zatman can be generalized by the concept of covariance matrix taper (CMT) [7]. In [8], a multi-parametric quadratic programming method is presented to control the null level of adaptive antenna array. The proposed algorithm can guarantee that the nulling level is strictly below the prescribed threshold. Recently, a

Received 11 June 2018, Accepted 16 August 2018, Scheduled 26 August 2018

* Corresponding author: Yifan Wu (wyfjgtm@126.com).

The authors are with the Engineer Optimization & Smart Antenna Institute, Northeastern University at Qinhuangdao, China. † Yifan Wu and Han Duan have made the same contributions on this paper.

large number of null broadening approaches [9–12] are proposed to improve the robustness against the mismatch scenarios. For example, in [9], the proposed algorithm utilizes the projection technique to preprocess the received data. And then, the diagonal loading (DL) method is used to get the new covariance matrix. It turns out that this approach can effectively broaden the null width and enhance the null depth even if the number of snapshots is limited. However, the choice of diagonal loading factor is a confusing problem. If the diagonal loading factor is extremely small, the improvement may seem to be minor, and it cannot suppress the effect of the noise. While if the loading factor is excessively large, it may lead to the fact that the nulls become shallow, which contributes to the degradation of the output signal-to-interference-and-noise ratio (SINR). A robust null broadening method based on uncertainty set and projection technique is presented in [11] to improve the robustness against array calibration errors. The presented method can be robust even though the calibration errors exist and its computational complexity is relatively low. In [12], a novel null broadening algorithm based on nulls optimization is proposed. The presented method can broaden the nulls efficiently as well as guarantee the gain of the desired signal. Unfortunately, all the methods mentioned above may not control the sidelobe level efficiently.

To further control the sidelobe level, several approaches have been proposed [13–17]. A modified MVDR beamformer is proposed by multiple additional quadratic inequality constraints outside the mainlobe beampattern area [13]. These constraints can ensure that the sidelobe level is strictly lower than the prescribed level. In [15], a blind beamforming algorithm based on the l_1 norm sparse constraint on the whole beam pattern is presented to suppress the sidelobe level. This method can effectively lower the sidelobe level and improve the SINR performance. This approach adds the sparse constraint equally on both the mainlobe and the sidelobe. However, the constraint should encourage dense distribution in the mainlobe and sparse distribution in the sidelobe. To further enhance the sidelobe control performance, a mixed norm constraint is proposed in [16]. The presented approach uses l_1 norm to encourage the sparse distribution on the sidelobe and l_∞ norm to encourage the dense distribution on the mainlobe. Recently, a novel sidelobe control method based on support vector machine regression (SVR) is widely used in the array signal processing.

The theory of SVR is initially introduced by Vapnik [17] based on the principle of structural risk minimization and is applied in a number of communications problems such as wireless sensor networks [18] and digital image processing [19]. Due to its improved generalization capabilities, it is widely employed in the array signal processing problems to control the sidelobe levels [20–24] and the antenna array synthesis problems [25–28]. The SVR-based beamforming algorithm is initially proposed [20] to improve the performance of MVDR. It utilizes the Vapnik insensitive function to serve as a penalty term to penalize the sidelobe level. The solution of the weight vector can be obtained via the quadratic programming (QP) technique. However, the computational complexity is not attractive. In [21], the iterative re-weighted least square (IRWLS) [29, 30] method is utilized to solve the SVR-based beamforming problem in order to save the computational cost. The SVR method is then used in [22] to suppress the sidelobe level of the Bayesian beamformer. An improved diagonal loading algorithm based on SVR is presented in [24]. These SVR-based approaches turn out to have a relatively low sidelobe level. Moreover, these methods can be robust under the steering vector mismatch scenarios. Another application of SVR is to deal with the antenna synthesis problems. It can be employed to perform a specific radiation pattern that meets the predefined requirements [25]. Because of its high accuracy, it can be a powerful method to design the array antenna. In [26], a novel three-dimensional (3D) antenna array modelling and synthesis technique based on SVR is presented. This technique can develop accurate two-dimensional (2D) and 3D models in the synthesis schemes with low complexity. A new accurate synthesis method based on the combination of the Methods of Moments (MoM) and SVR is presented in [27]. It combines the advantages of the SVR and MoM, and improves the performance of the SVR-based approach when there is a lack of training data.

This paper presents a novel beamforming algorithm for null broadening and sidelobe control. Initially, the covariance matrix is tapered based on Mailloux CMT algorithm to broaden the width of nulls for interference signals. Then, the original beamforming problem is formulated as a standard SVR problem to control the sidelobe level, which can be solved effectively through IRWLS procedure. This paper is organized as follows. Section 2 presents the data model and the conventional MVDR solution. The formulation of the proposed algorithm based on SVR is discussed in Section 3. In

Section 4, simulation results are presented to verify the performance of the proposed approach. Section 5 concludes the paper.

2. DATA MODEL

Consider a receiving array with M isotropic elements. The received data $\mathbf{x}(t) \in C^{M\times 1}$ of the antenna array at time t is given by

$$\mathbf{x}(t) = \mathbf{a}(\theta_0)s_0(t) + \sum_{j=1}^{J} \mathbf{a}(\theta_j)s_j(t) + \mathbf{n}(t) \tag{1}$$

where J stands for the number of interference signals. The signal and interference directions-of-arrival (DOAs) are θ_0 and $\theta_j\,(j = 1, 2, \ldots, J)$, respectively, with corresponding steering vectors $\mathbf{a}(\theta_0)$ and $\mathbf{a}(\theta_j)$. $s_0(t)$ and $s_j(t)$ are the signal and interference, respectively. $\mathbf{n}(t) = [n_1(t), \ldots, n_M(t)]^T$ with $n_i(t)$ representing the additive Gaussian noise of the ith sensor and the superscripts $(\cdot)^T$ denoting the transpose.

Let $\mathbf{R}_{xx} \in C^{M\times M}$ denote the theoretical covariance matrix of the array snapshot vector. Assume that $\mathbf{R}_{xx}$ is a positive definite matrix and it can be written as follows

$$\mathbf{R}_{xx} = \sigma_s^2\mathbf{a}(\theta_0)\mathbf{a}(\theta_0)^H + \sum_{j=1}^{J} \sigma_j^2\mathbf{a}(\theta_j)\mathbf{a}(\theta_j)^H + \sigma_n^2\mathbf{I} \tag{2}$$

where σ_s^2, σ_j^2 and σ_n^2 are the powers of the uncorrelated signals, interference and the noise. $(\cdot)^H$ denotes the conjugate transposition, and $\mathbf{I}$ is the identity matrix of M dimension.

The classical MVDR beamformer [4] is described as follows

$$\min_{\mathbf{w}} \ \mathbf{w}^H\mathbf{R}_{xx}\mathbf{w} \quad \text{subject to} \quad \mathbf{w}^H\mathbf{a}(\theta_0) = 1 \tag{3}$$

where $\mathbf{w} \in C^{M\times 1}$ is the weight vector of the array, and its solution $\mathbf{w}_{\text{MVDR}}$ can be expressed as

$$\mathbf{w}_{\text{MVDR}} = \frac{\mathbf{R}_{xx}^{-1}\mathbf{a}(\theta_0)}{\mathbf{a}^H(\theta_0)\mathbf{R}_{xx}^{-1}\mathbf{a}(\theta_0)}. \tag{4}$$

In practice, the exact covariance matrix is not available and is replaced by the sample covariance matrix $\hat{\mathbf{R}}_{xx}$, which can be expressed as follows

$$\hat{\mathbf{R}}_{xx} = \frac{1}{N}\sum_{l=1}^{N} \mathbf{x}(l)\mathbf{x}(l)^H \tag{5}$$

where N presents the number of snapshots.

3. ALGORITHM FORMULATION

In this section, the Mailloux CMT algorithm is initially utilized to widen the nulling extent. Then, the constraints are modified to control the sidelobe level. The objective function is further modified in order to ensure the existence of the admissible solution. The modified optimization problem is formulated as a standard SVR problem so that the sidelobe level is controlled effectively and the solution of the weight vector can be obtained efficiently.

3.1. Null Broadening

Assume that the narrowband interference signals impinging on the array are uncorrelated with each other as well as with the spatially white noise. According to [5], the terms in the covariance matrix $\mathbf{R}_{xx}$ are given by $R_{mn} = \sum_{j=1}^{J} \sigma_j^2 e^{j2\pi/\lambda(p_{ym}-p_{yn})\sin\theta_j} + \sigma_n^2\delta_{mn}$, where p_{ym} and p_{yn} stand for the location of the element. δ_{mn} is a Kronecker delta function. According to [5], we construct a cluster of q equal-power

incoherent signals around each original interfering signal to produce a notch of width W in each of the interference directions. In this case, the additional sources can be summed in closed form, as geometric sum and can be written as $\sum_{k=-\frac{K-1}{2}}^{\frac{K-1}{2}}(\sigma_j^2/K)e^{j2\pi/\lambda(p_{ym}-p_{yn})[\sin\theta_j+k\delta]} = \frac{\sin(K\Lambda_{mn})}{K\sin(\Lambda_{mn})}\sigma_j^2 e^{j2\pi/\lambda(p_{ym}-p_{yn})\sin\theta_j}$, where $\Lambda_{mn} = \frac{\pi(p_{ym}-p_{yn})\delta}{\lambda}$ and $\delta = \frac{W}{K-1}$. Therefore, each element in the covariance matrix can be rewritten as $\bar{R}_{mn} = R_{mn}\frac{\sin(K\Lambda_{mn})}{K\sin(\Lambda_{mn})}$. In matrix form, the Mailloux CMT can be expressed as

$$\bar{\mathbf{R}}_{xx} = \mathbf{R}_{xx} \circ \mathbf{T} \tag{6}$$

where "$\circ$" denotes Hadamard product, that is multiplying the corresponding elements of the two matrixes, and the form of matrix $\mathbf{T}$ can be written as $\mathbf{T} = (t_{mn})_{M\times M} = (\frac{\sin(K\Lambda_{mn})}{K\sin(\Lambda_{mn})})_{M\times M}$.

The CMT method can be expressed as the following optimization problem

$$\min_{\mathbf{w}} \ \mathbf{w}^H\bar{\mathbf{R}}_{xx}\mathbf{w} \quad \text{subject to} \quad \mathbf{w}^H\mathbf{a}(\theta_0) = 1. \tag{7}$$

The solution of the problem in Eq. (7) can be expressed as

$$\mathbf{w}_{\text{CMT}} = \frac{\bar{\mathbf{R}}_{xx}^{-1}\mathbf{a}(\theta_0)}{\mathbf{a}^H(\theta_0)\bar{\mathbf{R}}_{xx}^{-1}\mathbf{a}(\theta_0)} \tag{8}$$

where $\bar{\mathbf{R}}_{xx}$ is the tapered covariance matrix given by Eq. (6).

3.2. Sidelobe Control Based on SVR

The SVR is utilized to control the sidelobe level. Before the SVR is applied, all the variables mentioned above have to be transformed into real variables and the optimization problem also needs to be modified. The transformation of the original optimization problem into the standard SVR procedure can be shown as follows.

3.2.1. Data Preprocessing

a. Definition of the beamformer output: Consider a grid of DOAs θ_i, $i = 1, \ldots, P$, which sample the beampattern in $[-90°, 90°]$. Define an angular mainlobe beamwidth 2Δ centered at the assumed DOA θ_s. Using this sampled grid of DOAs, the desired beamformer output can be expressed as follows

$$d_i = \begin{cases} 0, & \text{if} \quad |\theta_i - \theta_s| > \Delta \\ 1, & \text{if} \quad |\theta_i - \theta_s| \le \Delta. \end{cases} \tag{9}$$

This definition takes into account a possible signal mismatch error up to Δ degrees. Thus, when the steering vector mismatch scenarios take place, the performance of the beamformer will not degrade seriously.

b. Real Variables Preprocessing: To utilize the proposed algorithm, all the complex variables mentioned above need to be modified into real variables. To this end, the array output power can be written as $\tilde{\mathbf{w}}^H\tilde{\mathbf{R}}_{xx}\tilde{\mathbf{w}}^H = \mathbf{w}^H\bar{\mathbf{R}}_{xx}\mathbf{w}$, where $\tilde{\mathbf{w}} \in R^{2M\times 1}$ and $\tilde{\mathbf{R}}_{xx} \in R^{2M\times 2M}$ can be expressed as follows

$$\tilde{\mathbf{w}}^T = \begin{bmatrix} \text{Re}(\mathbf{w}^T) & \text{Im}(\mathbf{w}^T) \end{bmatrix} \tag{10}$$

$$\tilde{\mathbf{R}}_{xx} = \begin{bmatrix} \text{Re}(\bar{\mathbf{R}}_{xx}) & -\text{Im}(\bar{\mathbf{R}}_{xx}) \\ \text{Im}(\bar{\mathbf{R}}_{xx}) & \text{Re}(\bar{\mathbf{R}}_{xx}) \end{bmatrix}. \tag{11}$$

Similarly, the beamformer output for each DOA can be rewritten in terms of real variables as $\mathbf{w}^H\mathbf{a}(\theta_i) = \tilde{\mathbf{w}}^T\tilde{\mathbf{a}}(\theta_i) + j\tilde{\mathbf{w}}^T\tilde{\mathbf{a}}'(\theta_i)$ in which θ_i, $i = 1, 2, \ldots, P$ is the candidate DOAs which sample pattern in $[-90°, 90°]$. $\tilde{\mathbf{a}}(\theta_i)$ and $\tilde{\mathbf{a}}'(\theta_i) \in R^{2M\times 1}$ are given by

$$\tilde{\mathbf{a}}(\theta_i)^T = \begin{bmatrix} \text{Re}(\mathbf{a}(\theta_i)^T) & \text{Im}(\mathbf{a}(\theta_i)^T) \end{bmatrix} \quad \tilde{\mathbf{a}}'(\theta_i)^T = \begin{bmatrix} \text{Im}(\mathbf{a}(\theta_i)^T) & -\text{Re}(\mathbf{a}(\theta_i)^T) \end{bmatrix}. \tag{12}$$

Define the real variables $\bar{\mathbf{a}}(i)$, and $\widetilde{d_i}$ as follows

$$\bar{\mathbf{a}}(i) = \begin{cases} \tilde{\mathbf{a}}(\theta_i), & i = 1, 2, \ldots, P \\ \tilde{\mathbf{a}}'(\theta_i), & i = P+1, P+2, \ldots, 2P \end{cases} \tag{13}$$

and

$$\widetilde{d}_i = \begin{cases} \mathrm{Re}(d_i), & i = 1, 2, \ldots, P \\ \mathrm{Im}(d_i), & i = P+1, P+2, \ldots, 2P. \end{cases} \tag{14}$$

Based on the definition of the real variables, the objective function can be rewritten as $\min \tilde{\mathbf{w}}^T \tilde{\mathbf{R}}_{xx} \tilde{\mathbf{w}}$.

3.2.2. Optimization Problem Modification for Sidelobe Control

a. Constraints Modification: The constraints of the conventional nulling broadening problem are equations. However, the sidelobe level is not attractive. To further control the sidelobe level, the constraints are modified as $|\tilde{\mathbf{w}}^T \bar{\mathbf{a}}(i) - \tilde{d}_i| \leq \varepsilon \, i = 1, 2, \ldots, 2P$, where ε defines the set of admissible beamformer solutions. In this paper, any beamformer whose outputs over the specified grid of DOAs are within an ε-band around the desired array output is an admissible solution. Among all admissible beamformers, the one with minimum output power would be the optimal solution of the problem.

b. Objective Function Modification: However, even if the number of inequality constraints is moderate, the set of admissible beamformers is likely to be empty. To solve this problem, a set of slack positive variables ξ_i, $\tilde{\xi}_i$ are introduced and the optimization problem is modified as follows

$$\begin{aligned} \min \quad & L(\tilde{\mathbf{w}}, \xi, \tilde{\xi}) = \frac{1}{2} \tilde{\mathbf{w}}^T \tilde{\mathbf{R}}_{xx} \tilde{\mathbf{w}} + C \sum_{i=1}^{2P} \left[(\xi_i)^m + (\tilde{\xi}_i)^m \right] \\ & \text{subject to} \begin{cases} \tilde{\mathbf{w}}^T \bar{\mathbf{a}}(i) - \tilde{d}_i \leq \varepsilon + \xi_i \\ -\tilde{\mathbf{w}}^T \bar{\mathbf{a}}(i) + \tilde{d}_i \leq \varepsilon + \tilde{\xi}_i \\ \xi_i, \tilde{\xi}_i \geq 0 \quad (i = 1, 2, \ldots, 2P) \end{cases} \end{aligned} \tag{15}$$

where $C \geq 0$ is a regularization constant, which sets a tradeoff between the output power term and a term that penalizes mismatches larger than ε. On the other hand, the exponent m can either be 1 or 2, which corresponds to linear ($m = 1$) and quadratic ($m = 2$) penalty, respectively. The optimization problem (15) can be reformulated to standard SVR problem based on the following lemma.

Lemma [31] The optimal solution of the problem in Eq. (15) is equivalent to the standard SVR problem, which can be expressed as follows

$$\min \quad J(\tilde{\mathbf{w}}) = \frac{1}{2} \tilde{\mathbf{w}}^T \tilde{\mathbf{R}}_{xx} \tilde{\mathbf{w}} + C \sum_{i=1}^{2P} L_\varepsilon^m(u_i) \tag{16}$$

where $u_i = |\tilde{d}_i - \tilde{\mathbf{w}}^T \bar{\mathbf{a}}(i)|$. The $L_\varepsilon^m(u)$ is a piecewise function whose value equals to $|u - \varepsilon|^m$ only if the condition $|u| \geq \varepsilon$ is satisfied. Otherwise, its value equals to 0.

Remarks. 1) According to the support vector machine terminology, the regularization term L_ε^m is the Vapniks ε-insensitive loss function (the value of m can either be 1 or 2). To sum up, the procedure can be interpreted as a regression problem for which the parameter ε defines the maximum gain level outside the mainlobe beampattern and therefore serves as a sidelobe control parameter.

2) The optimal solution of problem in Eq. (15) is equivalent to that of the problem in Eq. (16). The problem in Eq. (16) is a standard SVR problem, so it can be solved by the well-established QP method or IRWLS procedure. To reduce the computational complexity, the IRWLS method is selected to solve it.

3.2.3. Solution Based on IRWLS

The IRWLS procedure for solving SVR is initially introduced in [29]. Basically, the IRWLS procedure employs a quadratic approximation of the SVR loss function, which is shown to converge to true SVR solution. Initially, we perform a first-order Taylor series expansion of $L_\varepsilon^m(u)$, leading to $J(\mathbf{w}) = \frac{1}{2} \tilde{\mathbf{w}}^T \tilde{\mathbf{R}}_{xx} \tilde{\mathbf{w}} + C \sum_{i=1}^{2P} [L_\varepsilon^m(u_i^k) + \frac{\mathrm{d}L_\varepsilon^m(u)}{\mathrm{d}u}\Big|_{u_i^k} (u_i - u_i^k)]$, where $u_i^k = |\tilde{d}_i - \tilde{\mathbf{w}}_k^T \bar{\mathbf{a}}(i)|$ is the u_i at the kth iteration and $\tilde{\mathbf{w}}_k$ is the beamforming solution at the kth iteration. Then, a quadratic approximation

is constructed by imposing $J(\tilde{\mathbf{w}}_k) = J_2(\tilde{\mathbf{w}}_k)$ and $\nabla_{\tilde{\mathbf{w}}} J(\tilde{\mathbf{w}}_k) = \nabla_{\tilde{\mathbf{w}}} J_2(\tilde{\mathbf{w}}_k)$ where $\nabla_{\tilde{\mathbf{w}}}$ is the gradient operator with respect to the vector $\tilde{\mathbf{w}}$

$$J_2(\tilde{\mathbf{w}}) = \frac{1}{2}\tilde{\mathbf{w}}^T\tilde{\mathbf{R}}_{xx}\tilde{\mathbf{w}} + C\sum_{i=1}^{2P}\left[L_\varepsilon^m(u_i^k) + \frac{\mathrm{d}L_\varepsilon^m(u)}{\mathrm{d}u}\Big|_{u_i^k}\frac{(u_i^2)-(u_i^k)^2}{2u_i^k}\right] = \frac{1}{2}\tilde{\mathbf{w}}^T\tilde{\mathbf{R}}_{xx}\tilde{\mathbf{w}} + \frac{1}{2}\sum_{i=1}^{2P} f_i^m u_i^2 + b_i \quad (17)$$

where b_i denotes all the terms that do not depend on $\tilde{\mathbf{w}}$. On the other hand, the weights f_i^m depend on the particular penalty function: for the linear ($m = 1$) Vapniks ε-insensitive loss function, they are shown to be

$$f_i^1 = \frac{C}{u_i^k}\frac{\mathrm{d}L_\varepsilon^1(u)}{\mathrm{d}u} = \begin{cases} 0, & \text{if} \quad u_i^k < \varepsilon \\ \dfrac{C}{u_i^k}, & \text{if} \quad u_i^k \geq \varepsilon \end{cases} \quad (18)$$

and for the quadratic loss function ($m = 2$)

$$f_i^2 = \begin{cases} 0, & \text{if} \quad u_i^k < \varepsilon \\ \dfrac{2C(u_i^k - \varepsilon)}{u_i^k}, & \text{if} \quad u_i^k \geq \varepsilon. \end{cases} \quad (19)$$

As can be seen, the new quadratic cost function is a regularized least-squares cost function. Thus, its minimum value can be obtained by imposing $\nabla_{\tilde{\mathbf{w}}} J_2(\tilde{\mathbf{w}}) = 0$

$$\nabla_{\tilde{\mathbf{w}}} J_2(\tilde{\mathbf{w}}) = \tilde{\mathbf{R}}_{xx}\tilde{\mathbf{w}} - \sum_{i=1}^{2P} f_i^m\left(\tilde{d}_i - \tilde{\mathbf{w}}^T\bar{\mathbf{a}}(i)\right)\bar{\mathbf{a}}(i) = 0. \quad (20)$$

Equation (20) can be expressed in matrix form as

$$\nabla_{\tilde{\mathbf{w}}} J_2(\tilde{\mathbf{w}}) = \tilde{\mathbf{R}}_{xx}\tilde{\mathbf{w}} - \mathbf{\Phi}^T\mathbf{D}_f\tilde{\mathbf{D}} + \mathbf{\Phi}^T\mathbf{D}_f\mathbf{\Phi}\tilde{\mathbf{w}} = \mathbf{0} \quad (21)$$

where $\mathbf{\Phi} = [\bar{\mathbf{a}}(1), \bar{\mathbf{a}}(2), \ldots, \bar{\mathbf{a}}(2P)]^T \in R^{2P\times 2M}$, $\tilde{\mathbf{D}} = [\tilde{d_1}, \tilde{d_2}, \ldots, \tilde{d_{2P}}]^T \in R^{2P\times 1}$, $\mathbf{D}_f = \mathrm{diag}(f_1^m, f_2^m, \ldots, f_{2P}^m) \in R^{2P\times 2P}$, $\mathbf{0} \in R^{2M\times 1}$ is a column vector filled with 0. By solving Eq. (21), the weight vector can be expressed as follows

$$\tilde{\mathbf{w}} = [\tilde{\mathbf{R}}_{xx} + \mathbf{\Phi}^T\mathbf{D}_f\mathbf{\Phi}]^{-1}\mathbf{\Phi}^T\mathbf{D}_f\tilde{\mathbf{D}}. \quad (22)$$

The line search technique [32] is applied to speed up the convergence of the IRWLS algorithm, which is aimed to seek a descending direction as $\mathbf{p}_k = \tilde{\mathbf{w}}_s - \tilde{\mathbf{w}}_k$, with $\mathbf{w}_s$ being the minimum at each iteration of the weighted least-squares problem in Eq. (22). Then, the coefficients are modified along that direction as

$$\tilde{\mathbf{w}}_{k+1} = \tilde{\mathbf{w}}_k + \lambda_k\mathbf{p}_k \quad (23)$$

where $\lambda_k \in [0, 1]$ is the step size. Initially, the λ_k is set equal to 1, but if $J(\tilde{\mathbf{w}}_{k+1}) \geq J(\tilde{\mathbf{w}}_k)$, then it is iteratively reduced until observing a strict decrease in the function $J_2(\tilde{\mathbf{w}})$.

Once the new beamformer $\tilde{\mathbf{w}}_{k+1}$ is obtained, we calculate the error terms as $u_i = |\tilde{d}_i - \tilde{\mathbf{w}}_{k+1}^T\bar{\mathbf{a}}(i)|$ and update f_i^m until the algorithm achieves the prescribed convergence threshold δ. The whole IRWLS procedure is given in Table 1.

3.2.4. Summary of the Proposed Algorithm

The procedure of the proposed algorithm can be summarized as follows.

SVR-CMT Algorithm

(1) Collect data and estimate the covariance matrix $\hat{\mathbf{R}}_{xx}$ by Eq. (5) and the tapered covariance matrix $\bar{\mathbf{R}}_{xx}$ by Eq. (6).

(2) Compute the desired beamformer output d_i based on Eq. (15).

(3) Transform the complex variables including $\bar{\mathbf{R}}_{xx}$, d_i and $\mathbf{a}(\theta_i)$ into the real variables based on Eqd. (11)–(14) and obtain $\tilde{\mathbf{R}}_{xx}$, $\tilde{d}_i$ and $\bar{\mathbf{a}}(i)$. Meanwhile, prepare a $2M \times 1$ empty matrix for the weight vector $\tilde{\mathbf{w}}$.

(4) Obtain the weight vector $\tilde{\mathbf{w}}$ according to the IRWLS procedure given by Table 1, and transform the $\tilde{\mathbf{w}}$ to the complex variables $\mathbf{w}$ by Eq. (10).

Table 1. The IRWLS procedure.

Initialization: choose ε, C, and $m \in \{1, 2\}$. Set $k = 0$, $\tilde{\mathbf{w}}_0 = 0$, $u_i^0 = d_i$ and calculate f_i^m.
Repeat
Calculate $\tilde{\mathbf{w}}$ as (22) and set $\lambda_k = 1$.
Calculate $\tilde{\mathbf{w}}_{k+1} = \tilde{\mathbf{w}}_k + \lambda_k(\tilde{\mathbf{w}}_s - \tilde{\mathbf{w}}_k)$ as (23).
while $J(\tilde{\mathbf{w}}_{k+1}) \geq J(\tilde{\mathbf{w}}_k)$ **do**
reduce λ_k and calculate again $\tilde{\mathbf{w}}_{k+1}$.
end while
Set $k = k + 1$
Compute u_i^k with the obtained solution.
Update f_i^m using (18) for $m = 1$ or (19) for $m = 2$.
until Convergence when $\lvert J(\tilde{\mathbf{w}}_{k+1}) - J(\tilde{\mathbf{w}}_k)\rvert \leq \delta$

4. SIMULATION RESULTS

In this section, several simulations are constructed to evaluate the performance of the proposed method. Firstly, several evaluation indexes are defined as follows

a. The Beampattern: For the far-field signal $s(t)$ with DOA θ and steering vector $\mathbf{a}(\theta)$, the array output is $\mathbf{y}(t) = \mathbf{w}^H\mathbf{x}(t) = \mathbf{w}^H\mathbf{a}(\theta)s(t)$. The array response (output) is given by $F(\theta) = \mathbf{w}^H\mathbf{a}(\theta)$. According to the definition of the beampattern function, the expression of the beampattern function is shown as follows

$$G(\theta) \triangleq 20\text{lg}\left(\frac{|F(\theta)|}{\max|F(\theta)|}\right). \tag{24}$$

b. Output SINR: For an adaptive antenna array system, the output SINR is defined as the output signal power divided by the output interference-and-noise power. Normally, the dB is employed as the unit of the output SINR and it is given by $\text{SINR}_{\text{out}} \triangleq 10\text{lg}\frac{\mathbf{w}^H\mathbf{R}_s\mathbf{w}}{\mathbf{w}^H\mathbf{R}_{i+n}\mathbf{w}} = 10\text{lg}\frac{\sigma_0^2|\mathbf{w}^H\mathbf{a}(\theta_0)|^2}{\mathbf{w}^H\mathbf{R}_{i+n}\mathbf{w}}$, where $\mathbf{R}_s$ is the covariance matrix of the desired signal, and $\mathbf{R}_{i+n}$ is the covariance matrix of the interference-and-noise. The signal power σ_0^2 can be estimated by $\hat{\sigma_0^2} = \mathbf{w}^H\mathbf{R}_{xx}\mathbf{w}$.

In the following simulations, a uniform linear array (ULA) is exploited, which consists of ten isotropic sensors ($M = 10$) equispaced by half-wavelength. The DOA θ_0 of the desired signal and the DOAs (θ_1, θ_2) of the two interference signals are $\theta_0 = 0°, \theta_1 = -40°, \theta_2 = 40°$. The interference-to-noise ratio (INR) is set to 35 dB for both of the interference signals unless otherwise stated. The notch width W is assigned to 9°, and the number of the virtual interference signals K is set to 5. Sensor noises are simulated as spatially and temporally white Gaussian processes with zero mean and identical variances in each sensor. For the SVR parameters, it is assumed that the uncertainty region $\Delta = 2°$. In addition, the control parameters ε, C are set to 0.001 and 1, respectively. The angular range $[-90°, 90°]$ is uniformly sampled with $P = 60$ angles. Both the linear (L-SVR-CMT) and quadratic (NL-SVR-CMT) scenarios are plotted in the simulation results.

4.1. Experiment A Performance in the Absence of DOA Mismatches

In the following experiments, the DOA of the desired signal is exactly estimated, which means the DOA of the desired signal equals to the actual DOA. The beampattern, the output SINR performance versus the changing SNR and snapshots will be discussed in the following experiments.

4.1.1. A-1 The Beampattern Performance

In this experiment, the signal-to-noise ratio (SNR) of signal-of-interest (SOI) is assigned to 5 dB. 256 snapshots are used to compute the beampatterns of CMT and SVR-CMT (including L-SVR-CMT and

NL-SVR-CMT), which are plotted in Figure 1.

From Figure 1, we observe that when the DOA of the desired signal is exactly estimated, all the beampatterns generate deep and wide nulls at the DOAs of interference signals and maintain a distortionless response for the SOI. But the CMT method has a relatively high sidelobe level compared with the proposed method. That is because in the null broadening part, several virtual interference signals whose powers are small are used to replace the original interference, and it reduces the power of the interference. Therefore, the sidelobe level rises, and the depth of nulls decreases. The SVR-based algorithm can lower the sidelobe and generate deeper null levels at the DOAs of the interference. In this experiment, L-SVR-CMT has a generally higher performance compared with NL-SVR-CMT in terms of sidelobe level and the depth of nulls.

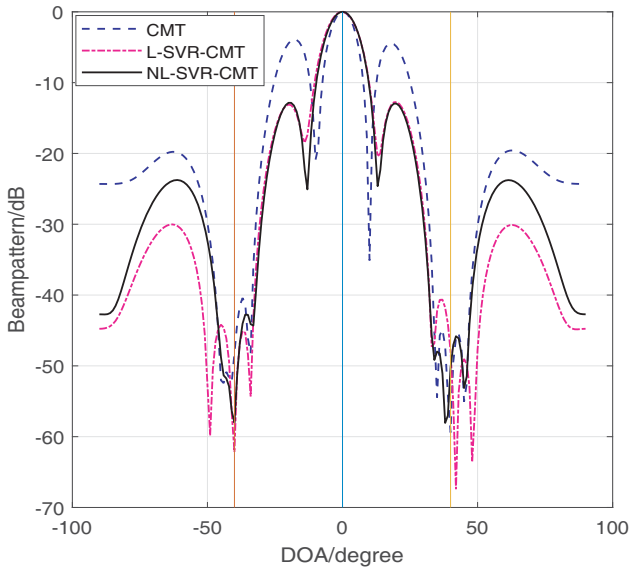

Figure 1. Beampattern under non-mismatch scenario.

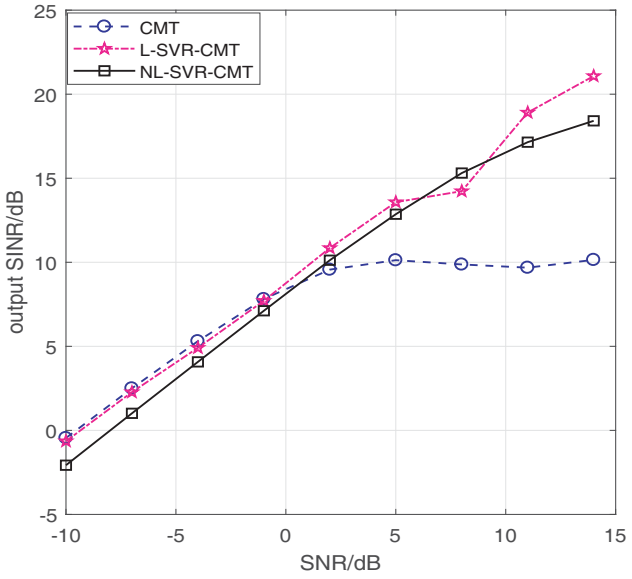

Figure 2. The output SINR versus the changing input SNR.

4.1.2. A-2 The Output SINR versus the Changing Input SNR

In this experiment, Figure 2 shows the array SINR curves of the aforementioned beamformers, based on 500 independent trials under the hypothesis that SNRs range from -10 dB to 15 dB, and the number of snapshots is fixed at 256. In this experiment, the INR of each interference signal is set to 30 dB.

As shown in the figure, compared with the conventional CMT method, the L-SVR-CMT has a generally higher output SINR within the whole range of input SNR. When the input SNR > 2 dB, the performance of NL-SVR-CMT surpasses the CMT.

4.1.3. A-3 The Output SINR versus the Changing Snapshots

In this experiment, Figure 3 gives the array SNIR curves of the aforementioned beamformers, based on 500 independent trials under the condition that the snapshots range from 25 to 1024. The input SNR is assigned to 20 dB.

From Figure 3, it can be seen that the output SINR of SVR-CMT algorithm is higher than that of CMT. That is because when the SNR is 20 dB, the desired signal dominates the covariance matrix, thus using the covariance matrix to replace the interference-and-noise covariance matrix is not precise enough. Thus, the performance of CMT may degenerate and it may cause the dissatisfied beampatterns, such as the rise of sidelobe level. Fortunately, for the proposed method, the ε-insensitive function serves as a sidelobe controller, thus it can improve the beamforming performance effectively.

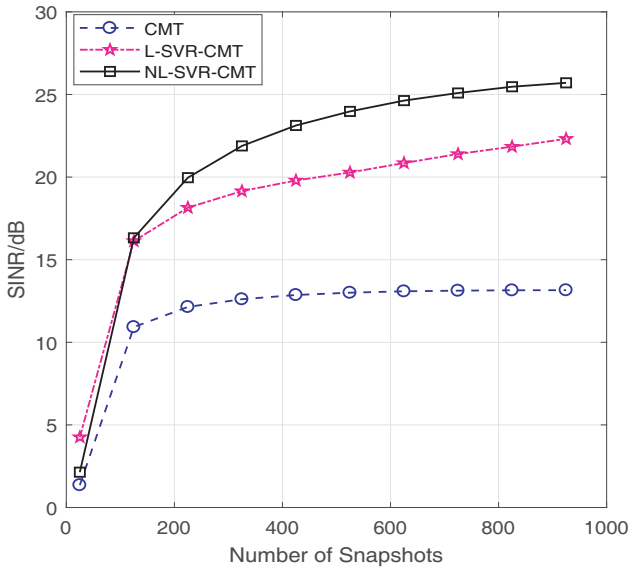

Figure 3. The output SINR versus the changing snapshots.

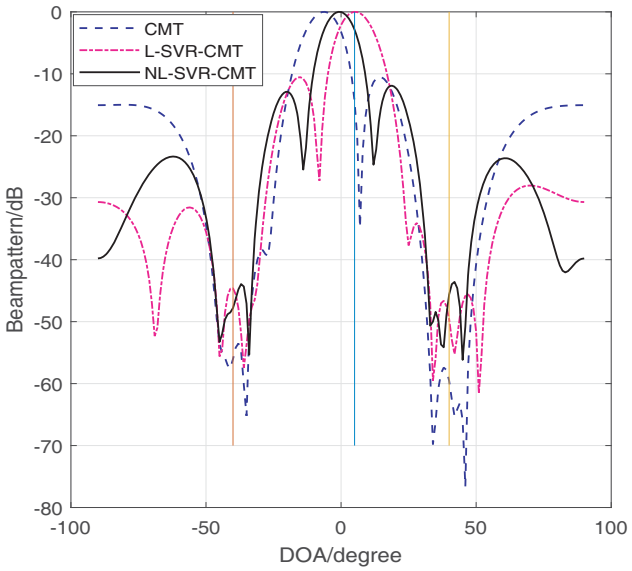

Figure 4. Beampattern under 5° mismatch scenario.

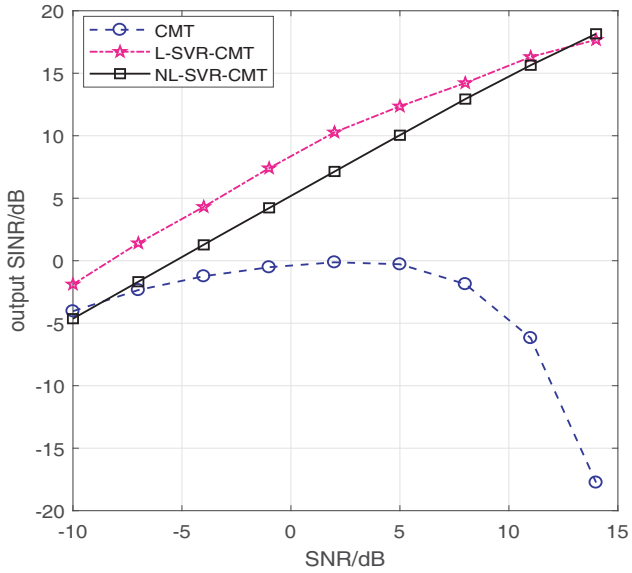

Figure 5. Output SINR versus input SNR under 5° mismatch scenario.

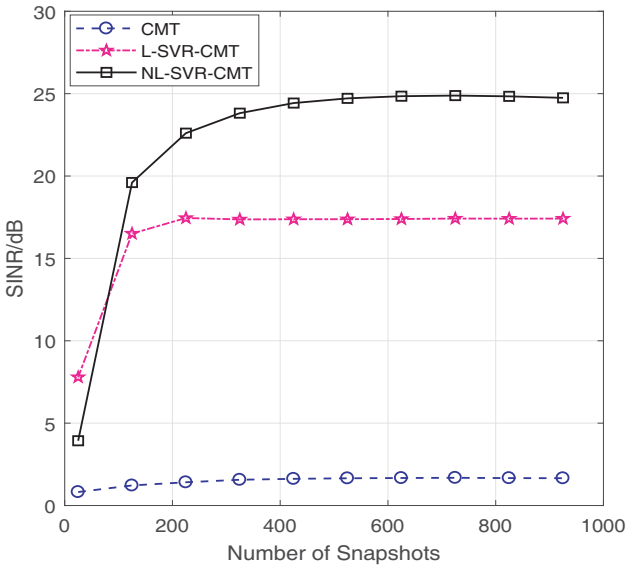

Figure 6. Output SINR versus snapshots under 5° mismatch scenario.

4.2. Experiment B Performance in the Situation of DOA Mismatches

In the following experiments, the performance of the proposed method for the DOA mismatch problem is simulated. Except for the DOA θ_0, other simulation parameters are identical to those in the previous simulations. Figure 4–Figure 6 depict the beampatterns and SINR performance of the aforementioned methods with $\Delta\theta_0 = 5°$ (assume that the desired signal arrives actually from 5°, however, the DOA estimation is equal to $\theta_0 = 0°$).

4.2.1. B-1 The Beampattern Performance

In this experiment, Figure 4 gives the beampattern of CMT and SVR-CMT. Although the CMT method generates deep nulls in the direction of interferences, it has an unacceptable beampattern since it results in mainlobe shifting or sidelobe rising by a big margin. Fortunately, the proposed method, especially the L-SVR-CMT, has a generally better performance in terms of mainlobe direction and the sidelobe level. Therefore, the presented method improves the beamforming performance when the DOA estimation is not precise enough.

4.2.2. B-2 The Output SINR Performance

Figure 5 and Figure 6 show the output SINR versus input SNR and changing snapshots for the DOA mismatch scenario, respectively. From Figure 5, the SINR performance of the CMT method degenerates when the SNR is higher than 5 dB. In Figure 6, its SINR is around 0 dB, and it does not increase even if the number of snapshots increases. That is because when the mismatch scenarios take place, the CMT method treats the desired signal as interference signal, especially in the high SNR scenarios. On the other hand, the proposed method has a better SINR performance than that of CMT. That is because when we define the desired beamformer response, the DOAs are sampled in $[-90°, 90°]$. Thus, even if the DOA estimation is not precise enough, the error can be mollified by the SVR training. Therefore, the proposed method can improve the SINR performance when the DOA estimation error exists.

To fairly evaluate the efficiency of the proposed method, its computational complexity should be analysed. According to the previous analysis, the computational complexity of the proposed method mainly includes: (1) the covariance matrix taper according to Equation (6), of order $O(M^2)$ generated by Hadamard product, where M is the number of array elements; (2) the IRWLS procedure to solve the weight vector iteratively according to Eq. (22). At each iteration, the proposed algorithm needs to solve a linear system of $2M$ equations with $2M$ unknowns, in order to obtain Eq. (22). Therefore, the computational complexity of the proposed method is, basically, *Number of Iterations* $\times O((2M)^3)+O(M^2)$. According to our observation, the number of iteration is usually small. Typically, it is no more than 2. Thus, when $M \gg 8$, the computational complexity order of the proposed method is $O(M^3)$. The CMT procedure includes the covariance matrix inversion and covariance taper, so its computational complexity is $O(M^3)+O(M^2)$, and its order is $O(M^3)$. Thus, when $M \gg 8$, the proposed method has the same order of computational complexity compared with CMT method, so it does not increase the computational complexity significantly. The comparison of the computational complexity can be seen in Table 2.

Table 2. Comparison of the computational complexity.

Methods	Covariance Matrix Taper	Inverse
CMT	$O(M^2)$	$O(M^3)$
SVR-CMT	$O(M^2)$	$O(8M^3)$

5. CONCLUSIONS

This paper presents an effective beamforming method based on SVR for null broadening and sidelobe control. The original beamforming problem is formulated as a standard SVR problem so that the beamforming can be controlled effectively, and the solution of the weight vector can be obtained efficiently. Compared with the previous works, the proposed approach can effectively control the sidelobe and nulling level. At the same time, it can improve the output SINR performance even if the DOA error exists. Simulation results are presented to verify the performance of the proposed SVR-CMT beamformer with robustness and relatively good beamforming performance.

ACKNOWLEDGMENT

This work was supported by the Natural Science Foundation of Hebei Province (No. F2016501139), and by the Fundamental Research Funds for the Central Universities under Grant (Grant No. N172302002, Grant No. N162304002), and by the National Natural Science Foundation of China (Grant No. 61501102).

REFERENCES

1. Chen, C. and W. B. Cai, "Low complexity beamforming and user selection schemes for 5G MIMO-NOMA systems," *IEEE Journal on Selected Areas in Communications*, Vol. 35, No. 12, 2708–2722, 2017.
2. Wang, L. and C. Andrea, "Microphone-array ego-noise reduction algorithms for auditory micro aerial vehicles," *IEEE Sensors Journal*, Vol. 17, No. 8, 2447–2455, 2017.
3. Hassanien, A. and G. Moeness, "Dual-function radar-communications: Information embedding using sidelobe control and waveform diversity," *IEEE Transactions on Signal Processing*, Vol. 64, No. 8, 2168–2181, 2016.
4. Capon, J., "High resolution frequency-wavenumber spectrum analysis," *Processing of IEEE*, Vol. 57, No. 58, 1408–1418, 1969.
5. Mailloux, R. J., "Covariance matrix augmentation to produce adaptive array pattern roughs," *Electronics Letters*, Vol. 31, No. 10, 771–772, 1995.
6. Zatman, M., "Production of adaptive array troughs by dispersion synthesis," *Electronics Letters*, Vol. 31, No. 25, 2141–2142, 1995.
7. Guerci, J. R., "Theory and application of covariance matrix tapers for robust adaptive beamforming," *IEEE Transactions on Signal Processing*, Vol. 47, No. 4, 977–985, 1999.
8. Liu, F., J. Wang, C. Y. Sun, and R. Du, "Robust MVDR beamformer for nulling level control via multi-parameteric quadratic programming," *Progress In Electromagnetics Research C*, Vol. 20, 239–254, 2011.
9. Li, W. X., X. J. Mao, and Y. X. Sun, "A new algorithm for null broadening beamforming," *Journal of Electronics and Information Technology*, Vol. 36, No. 12, 2882–2888, 2014.
10. Mao, X. J., W. X. Li, and Y. S. Li, "Robust adaptive beamforming against signal steering vector mismatch and jammer motion," *International Journal of Antennas and Propagations*, Vol. 10, 1–12, 2015.
11. Zhao, Y., W. X. Li, X. J. Mao, and N. Zhang, "Null broadening beamforming against array calibration errors," *Journal of Harbin Engineering University*, Vol. 39, No. 1, 163–168, 2018.
12. Li, S., "Robust beamforming algorithm based on nulls optimization," *Signal Processing*, Vol. 33, No. 12, 1542–1547, 2017.
13. Liu, J., A. B. Gershman, and Z. Q. Luo, "Adaptive beamforming with sidelobe control: A second-order cone programming approach," *IEEE Signal Processing Letters*, Vol. 10, No. 11, 331–334, 2013.
14. Zaharis, Z. D., C. Skeberis, and T. D. Xenos, "Improved antenna array adaptive beamforming with low side lobe level using a novel adaptive invasive weed optimization method," *Progress In Electromagnetics Research*, Vol. 124, 137–150, 2012.
15. Huang, J., P. Wang, and Q. Wan, "Sidelobe suppression for blind adaptive beamforming with sparse constraint," *IEEE Communications Letters*, Vol. 15, No. 3, 343–345, 2011.
16. Liu, Y. and Q. Wan, "Sidelobe suppression for robust beamformer via the mixed norm constraint," *Wireless Personal Communications*, Vol. 65, No. 4, 825–832, 2012.
17. Vapnik, V. N., *Statistical Learning Theory*, Wiley, New York, 1998.
18. Salah, Z., M. Tarek, and A. Bechir, "Fault detection in wireless sensor networks through SVM classifier," *IEEE Sensors Journal*, Vol. 18, No. 1, 340–347, 2018.

19. Islam, M., G. Mallikharjunudu, A. S. Parmar, A. Kumar, and R. H. Laskar, "SVM regression based robust image watermarking technique in joint DWT-DCT domain," *2017 International Conference on Intelligent Computing, Instrumentation and Control Technologies*, 1426–1433, 2017.
20. Ramon, M. M., N. Xu, and C. G. Christodoulou, "Beamforming using support vector machines," *IEEE Antennas and Wireless Propagation Letters*, Vol. 4, No. 1, 439–442, 2005.
21. Cesar, C. G. and S. Ignacio, "Robust array beamforming with sidelobe control using support vector machines," *IEEE Transactions on Signal Processing*, Vol. 55, No. 2, 574–584, 2007.
22. Lu, Y., J. An, and X. Bu, "Adaptive bayesian beamforming with sidelobe constraint," *IEEE Communications Letters*, Vol. 14, No. 5, 369–371, 2010.
23. Cui, L., Y. Li, and X. Li, "Application of support vector regression in beamforming," *International Conference on Computer Science and Network Technology*, 1270–1273, 2012.
24. Lin, C., Y. A. Li, Y. Y. Fang, and X. J. Bai, "The robust diagonal loading beamforming method using support vector machines," *Acta Armamentarii*, Vol. 34, No. 5, 598–604, 2013.
25. Ayestaran, R. G. and F. Las-Heras, "Support vector regression for the design of array antennas," *IEEE Antennas and Wireless Propagation Letters*, Vol. 4, No. 1, 414–416, 2005.
26. Ayestaran, R. G. and F. Las-Heras, "Support vector multi-regression and equivalent 2D modelling for 3D antenna array synthesis," *European Conference on Antennas and Propagation*, 1–5, 2008.
27. Ayestaran, R. G., J. Laviada, and F. Las-Heras, "Realistic antenna array synthesis in complex environments using a MOM-SVR approach," *Journal of Electromagnetic Waves and Applications*, Vol. 23, No. 1, 97–108, 2009.
28. Martinez-Ramon, M. and C. Christodoulou, "Support vector machines for antenna array processing and electromagnetics," *Synthesis Lectures on Computational Electromagnetics*, 1–120, 2006.
29. Pérez-Cruz, F., "An IRWLS procedure for SVR," *The 10th European Signal Processing Conference*, 1–4, 2000.
30. Pérez-Cruz, F., C. Bousoño-Calzón, and A. Artés-Rodríguez, "Convergence of the IRWLS procedure to the support vector machine solution," *Neural Computation*, Vol. 17, 7–18, 2005.
31. Sun, D. S., "The researches on support vector machine classification and regression methods," *Central South University*, 49–50, 2004.
32. Nocedal, J. and S. J. Wright, *Numerical Optimization*, Springer-Verlag, New York, 1999.